J Therm Spray Tech (2019) 28:1199–1211
https://doi.org/10.1007/s11666-019-00882-0

PEER REVIEWED

Pores Structure Change Induced by Heat Treatment in Cold-Sprayed Ti6Al4V Coating

Hongxia Zhou[1,2] · Chengxin Li[1] · Hao Yang[1] · Xiaotao Luo[1] · Guanjun Yang[1] · Wenya Li[3] · Tanvir Hussain[4] · Changjiu Li[1]

Submitted: 30 December 2018 / in revised form: 1 May 2019 / Published online: 24 June 2019

Abstract In this study, the evolution of pores structure in cold-sprayed Ti6Al4V coating (TC4) was analyzed before and after 600-1100 °C heat treatment. It was found that almost no change happened to pores under the heat treatment temperature below 600 °C. When the heat treatment temperature was increased to 700 °C, the coating recrystallized, and pores turned to spheroid and healed because of the "bridging" effect. Some of the pores coarsened after 800 °C and 900 °C heat treatment. This kind of phenomenon grew severer when the heat treatment temperature increased to 1000 °C and 1100 °C. On the whole, with the increment of temperature, for the coating prepared at relatively low temperature, apparent porosity measured by image analysis method tended to go down first and then up, but it decreased all the time for the coating prepared at relatively high temperature. The reason for this phenomenon was contributed to the bonding state of particles in the coating. Only when there were fewer weakly bonded interfaces, the detachment between the particle interfaces which may be caused by release of residual stress did not occur, and there was no pores expansion and internal connectivity, so the porosity continuously decreased.

Keywords cold spraying · heat treatment · porosity · quasi-in situ · Ti6Al4V

✉ Chengxin Li
licx@mail.xjtu.edu.cn

[1] State Key Laboratory for Mechanical Behavior of Materials, School of Materials Science and Engineering, Xi'an Jiaotong University, Xi'an 710049, Shaanxi, People's Republic of China

[2] Qinghai Provincial Key Laboratory of New Light Alloys, Qinghai Provincial Engineering Research Center of High Performance Light Metal Alloys and Forming, Qinghai University, Xining 810016, People's Republic of China

[3] State Key Laboratory of Solidification Processing, Northwestern Polytechnical University, Xi'an 710072, People's Republic of China

[4] Faculty of Engineering, University of Nottingham, Nottingham NG7 2RD, UK

Introduction

Cold spraying is an emerging thermal spray technology that can accelerate particles to supersonic speed and impact onto a substrate in their solid state (Ref 1-3). The formation of coating mainly depends on the plastic deformation of particles (Ref 4). In the beginning, ductile materials like Al (Ref 5, 6), Cu (Ref 7, 8) and Sn (Ref 9) were deposited as they can be easily deformed when impacted on substrate material. With the development of technology, it is of growing interest to deposit other materials with this approach including Ti and Ti alloys (Ref 10-12), superalloys (Ref 13-15) and even ceramic materials (Ref 16-18). Due to relatively low operating temperature, cold spraying is more suited to spray temperature-sensitive materials like Ti and Ti alloys that are prone to oxidation at the temperature above 600 °C. During the past decades, there have also been reports of Ti and Ti alloy cold-sprayed coatings. Many studies showed that the coating exhibited a porous microstructure, and it was difficult to obtain a dense Ti and Ti alloy coating when using nitrogen as the propellant gas. Up to now, the porosity of the cold-sprayed Ti or its alloy coatings was reported as 5-25% depending on the spray conditions, while with a relatively high deposition efficiency (usually > 50%) (Ref 19, 20). Since pores formed between the weakly bonded particles in cold-sprayed coating, they can reveal inter-particle bonding level to a

large extent. As porosity determines the coating performance, especially the large pores, they significantly deteriorate mechanical, physical and electrical properties (Ref 21). Many efforts have been taken to decrease the porosity in Ti and its alloys. These efforts can be classified into two categories: (I) changing spraying parameters including gas species, temperature, pressure, standoff distance and so on, aimed to increase the kinetic energy of the powder particle and enhance plastic deformation; and (II) regulating powder state including designing new powder, preheating and softening the particles to decrease the resistance to plastic deformation during impact. In recent years, many studies have found that the post-treatment of cold-sprayed coating can eliminate pores existing between the poorly bonded particles. Sundararajan et al. (Ref 22) studied the effect of a post-spray heat treatment at various temperatures on Cu, Ag, Zn, Nb, Ta, Ti and 316L stainless steels cold-sprayed coatings; the results showed that the heat treatment of the cold spray coatings causes a decrease in the extent of inter-splat cracking and porosity in the case of all the coatings. Hussain et al. (Ref 23) used a mercury intrusion porosimetry method to quantify and characterize the porosity of cold-sprayed titanium deposits; they found that the interconnected porosity decreased after heat treatment at 1050 °C for 60 min. Garrido et al. (Ref 24) showed that the porosity of TC4 coating decreased after a solution and precipitation heat treatment at 1000 °C for 1 h and 537 °C for 4 h, respectively. But this was not always the case. Li et al. (Ref 25) showed that the porosities of Ti and Ti-6Al-4V coatings were apparently increased owing to the coalescence of incomplete interfaces or the appearance of submicron pores. Similar results had been observed in cold-sprayed TC4 after heat treatment (Ref 26).

In addition, post-spray heat treatment has been shown to be an effective method to optimize the microstructure and properties of cold-sprayed coatings. However, prior studies paid more attention on the effect of the heat treatment to the mechanical property of cold-sprayed Ti and Ti alloys coating; the evaluation of the pores structure after heat treatment was very limited. Nevertheless, the changes of pores structure in cold-sprayed Ti and Ti alloys are also very important, as the porosity determines the coating performances including conductivity, cohesive strength and corrosion resistance. Properties of the coating can be speculated with the variation of pores. Thus, it is important to analyze the effort of annealing treatment on pore structure of the cold-sprayed Ti alloys coatings.

In this study, the evolution of microstructure of cold-sprayed TC4 coating before and after different heat treatment temperature was observed using quasi-in situ technology, and the porosity evolution mechanism was also analyzed systematically.

Experimental

TC4 coatings were deposited onto commercial TC4 bulk substrate with the aim of studying the reliability of these coatings deposited by cold spraying for repairing components of the same alloy. Plasma-atomized TC4 powder (Raymor Industries Inc., Boisbriand, Canada) was used as the starting powder, and the particle size ranges from $\sim +15$ to ~ -30 μm with a mean value of $\sim$ 22.6 μm. The coatings were prepared using an in situ shot-peening-assisted cold spraying technology, and 1Cr18 stainless steel was used as shot peening particles with a size distribution from $\sim +125$ to ~ -300 μm and a mean value of $\sim$ 181 μm. Both TC4 and shot peening particles were mechanically mixed as spraying feedstock. The coatings were prepared using an in-house cold spraying system, model number CS-2000. In this system, the spray powders are fed along the axis of a convergent–divergent nozzle with throat and outlet diameters and length of divergent section of 2.7, 6 and 150 mm, respectively. Nitrogen was used as the propellant gas and powder carrier gas, and the inlet temperature of the gas was 550-750 °C with the interval of 50 °C; the spraying parameters are shown in Table 1. The thickness of the coating was about 1 mm.

Scanning electron microscopy (FESEM) (TESCAN MIRA3, Czech) was carried out to characterize the microstructure of the as-sprayed and heat treatment coatings. The sawed sample with a size of $10 \times 5 \times 5$ mm was ground by SiC abrasive paper and finally polished by a 0.1-μm diamond polishing agent. The samples were then ultrasonically cleaned twice in an ethanol bath for 5 min to remove the adhered polishing agent; then, the samples were placed in a quartz tube, which was evacuated to 7×10^{-4} Pa with a molecular pump to avoid oxidation and then sealed. After that, the vacuum tube was heated at an identical heating rate of 5 °C/min over a wide range of temperatures (600, 700, 800, 900, 1000 and 1100 °C) for the duration of 2 h in a chamber furnace. Following heat treatment, the quartz tube was air-cooled to room temperature. The microstructure of the coating was observed using a quasi-in situ method by which the same microstructure in the coating before and after heat treatment was observed using SEM. At 200x magnification, we measured the distance between two points at the boundary of a particle in the as-sprayed coating, recorded as d_0 (about 500 ± 100 μm). After heat treatment, the distance between the same two points was measured again, denoted as d_1; the difference $d_0 - d_1$ is the distance reduction. The distance difference per 100 microns was used to measure the volume change of coating after heat treatment.

Table 1 Spraying parameters of TC4 coatings

Gas	Gas inlet temperature, °C	Gas pressure, MPa	Gun traverse speed, mm/s	Standoff distance, mm	Powder feeder rate, g/min	Content of shot peening particle, vol.%
N_2	550-750	3	40	20	50	70

The porosities of specimens before and after heat treatment were measured from the cross section of coatings based on image analysis. Ten SEM images were recorded at 1000 × in backscattered electron mode for each sample. Archimedes water immersion method was also used to measure the density of the cold-sprayed TC4 coating. Three measurements of sample weight in air and in a bath of distilled water at room temperature were made using a 4-decimal point balance. The volume fraction of porosity was then calculated from $1 - \rho_m/\rho_t$, where ρ_m is the measured density and $\rho_t = 4.506$ g/cm^3, the theoretical density of TC4.

The residual stresses of the coating prepared at 550 °C before and after heat treatment were analyzed by the x-ray diffraction method, which was conducted on the D8-Discover (Bruker AXS Inc. Madison, WI, USA) with Cu K_α radiation source. The "Sin$^2\Psi$" method of stress determination (Ref 27) was applied, using reflection from Ti (213) crystal planes with elastic constants $E = 110$ GPa and Poisson ratio $\gamma = 0.31$, and 11 sample tilts from $\Psi = 0°$ to 60°. The residual stress acting in the direction perpendicular to the spraying direction was calculated. The experimental schematic of the x-ray diffraction can be found elsewhere (Ref 28).

Results and Discussion

Microstructure Evolution

The quasi-in situ micrograph of as-sprayed five TC4 coatings and the coatings after 600 °C heat treatment is presented in Fig. 1. (The spray temperature is shown at the top of the figure, and so are the following figures.) By comparing the two sets of pictures, it was found that the coatings did not change much after heat treatment of 600 °C except some regions as denoted which may be resulted from evaporation of residual impurity in vacuum environment. In addition to this, the micrograph of five coatings before and after heat treatment was almost the same, and the particle boundaries were still very clear. In the coating prepared at relatively low temperature, the spherical particles can be seen clearly accounting for the slight deformation (Ref 29). Besides, there were some tiny pores that had disappeared, and no spheroidization of the pores was observed. This indicated that the diffusion of atoms was low at this temperature.

When the heat treatment temperature was increased to 700 °C, the microstructure of the coating began to change from the quasi-in situ observation as shown in Fig. 2. An important change was the recrystallization of the coating, which can be seen from the locally magnified morphology of the 700 °C sprayed coating, a large number of equiaxial grains appeared on the surface of the coating, and the boundary between particles was blurred due to recrystallization. Another important change was the spheroidization of the pores, as indicated by the red arrows. This was consistent with what has been reported in the literature (Ref 30). In the enlarged picture, the interface between the particles was partially healed, a small gap left by the partially visible interface that had not completely healed (as shown by the red circles). The spheroidization mechanisms of the pores will be further discussed later. Since the particles were plastically deformed during the cold spraying process, recrystallization occurred in the process of subsequent heat treatment, which has been confirmed by numerous reports (Ref 25, 29, 31-33). For the severe impact of particles during cold spraying, there were a large number of dislocations clustering on the particle interface, and recrystallized grains tended to nucleate preferentially in these regions of high energy (Ref 34). Nucleation and growth of recrystallized grains prompted the surface of the particles to grow undulation. Since the flat particle interface was composed of two mutually contacting particle surfaces, roughening of the two caused point contact to occur at some locations, thereby forming a "bridging" (Ref 35) (as the black arrows shown in Fig. 3(a)). It was the "bridge" effect that gradually healed particle interfaces (as the white arrows shown in Fig. 3(b)). The recrystallization of the coating caused the surface of particles to obscure and disappear, and also caused a large number of tiny pores to close, and the porosity of the coating decreased significantly. (The porosity will be shown in a later section.) The elimination of particle boundaries and the formation of grain boundaries across these eliminated boundaries were an indication that improved metallurgical bonding has been obtained (Ref 36).

Figure 4 shows the quasi-in situ microstructure of the coatings before and after heat treatment at 800 °C. It can be seen that the interfaces between the particles further

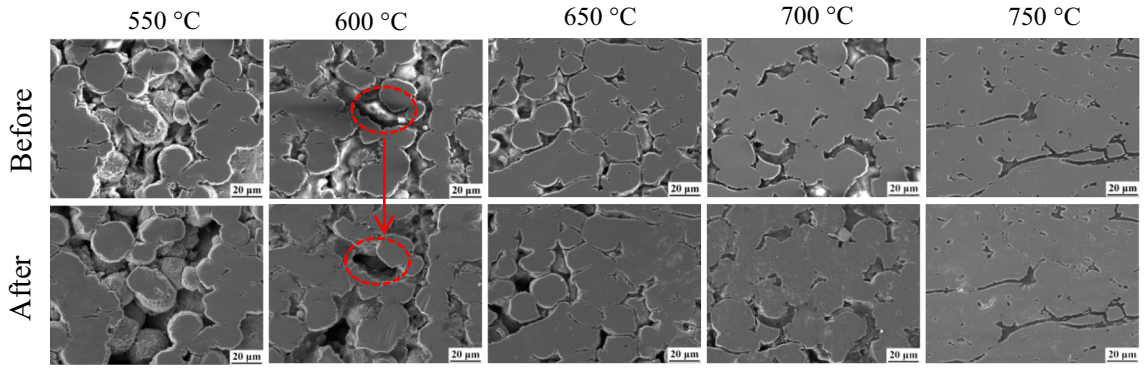

Fig. 1 Quasi-in situ observation of coatings before and after 600 °C heat treatment

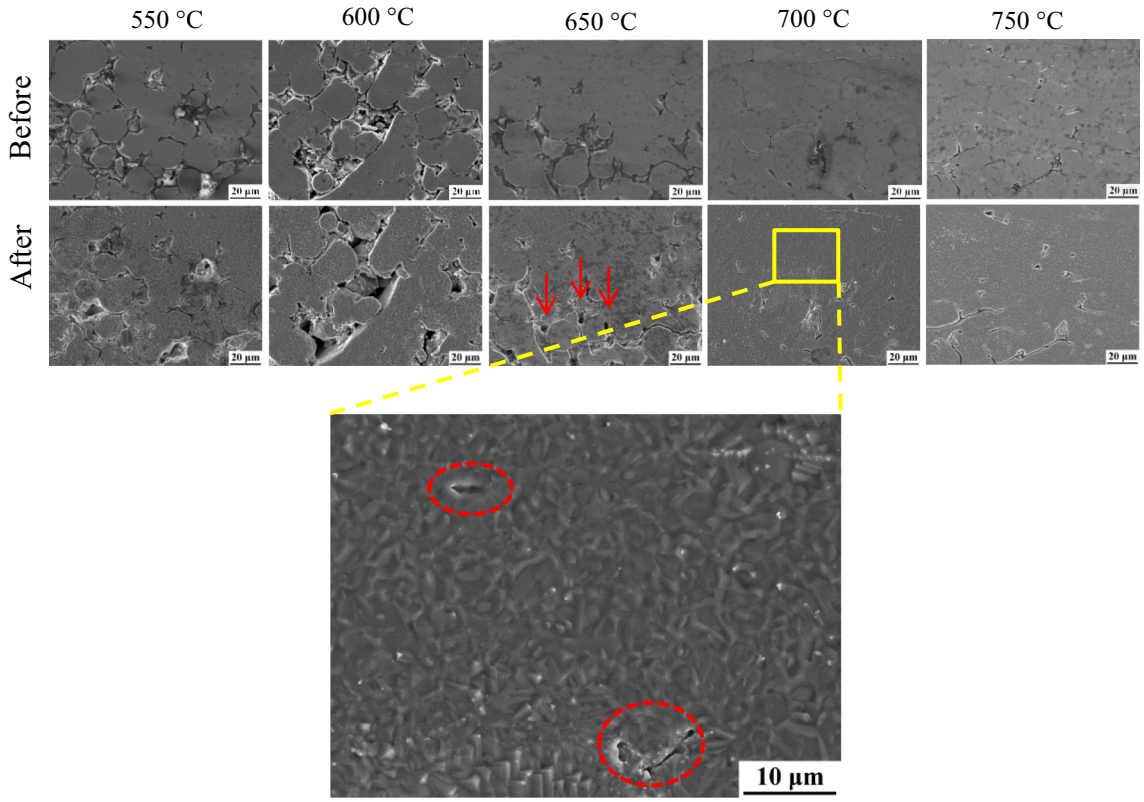

Fig. 2 Quasi-in situ observation of coatings before and after 700 °C heat treatment

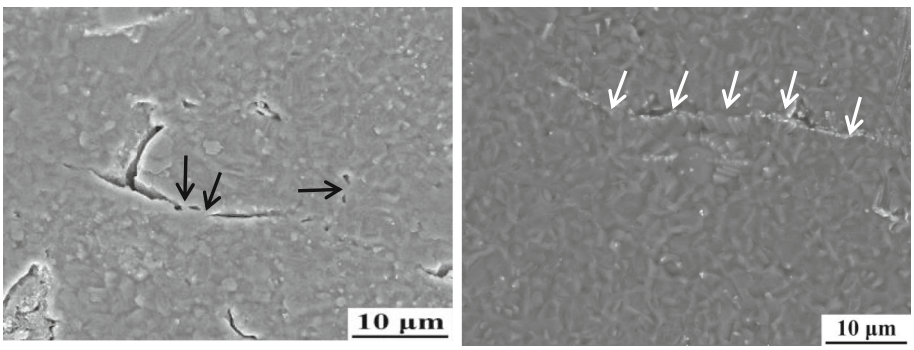

Fig. 3 Interfacial bridging (a) and healing (b) in 700 °C coating after 700°C heat transfer

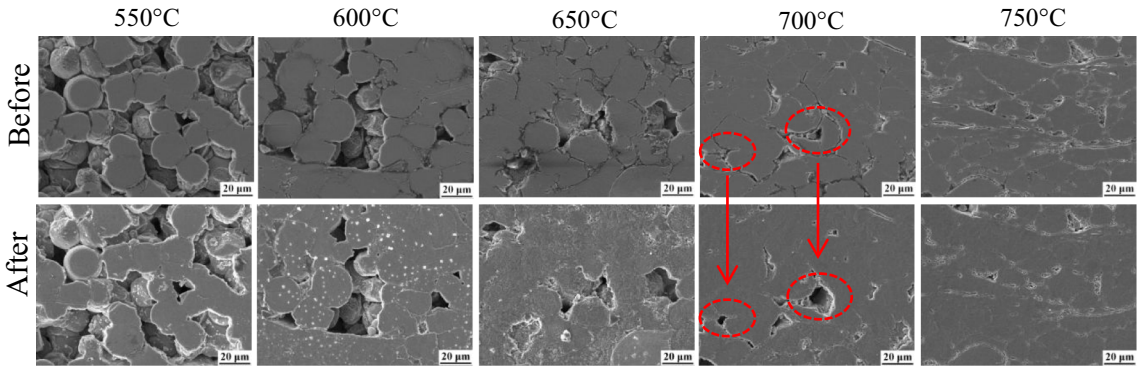

Fig. 4 Quasi-in situ observation of coatings before and after 800 °C heat treatment

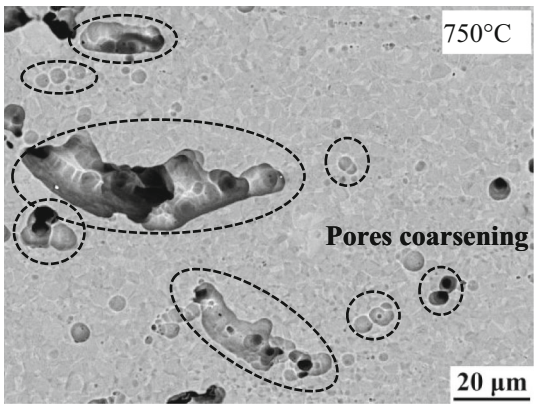

Fig. 5 Pores coarsening in 750 °C coating after 800 °C heat treatment

disappeared after heat treatment at 800 °C, and coarsening of the pores was partially observed (shown by red circles), which indicated that atomic diffusion was further improved at this temperature (Ref 32, 37). The reason for the coarsening of the pores was movement and mutual connection of the pores caused by diffusion at a high temperature (Ref 38). After the coating prepared at 750 °C was ground and polished with a method for preparing metallographic samples, pores coarsening is clearly observed in Fig. 5.

Figure 6 shows the quasi-in situ microstructure of the coatings before and after vacuum heat treatment at 900 °C. Similar to the 800 °C heat treatment, there was evidence of pores and gap enlargement in some coatings. In addition, in the dense coating of 700 and 750 °C, the particles interface further disappeared due to increased diffusion.

Figure 7 shows the quasi-in situ microstructure of the coatings before and after 1000 °C heat treatment. It can be seen that the coating microstructure underwent a greater change after vacuum heat treatment at 1000 °C. The particles interface was completely absent in the five coatings. Pore expansion and microstructure collapse were observed in the 650 °C coatings. A lot of pores have disappeared, and spheroidization of the pores was observed in the 700 °C coating (shown by red arrows). Since the temperature is close to the β phase transition temperature, the surface embossing caused by the phase transformation made the surface of the samples rough. On the other hand, since the diffusion coefficient of atoms in the β phase is large, the thermal diffusion was enhanced at this temperature, which led to an increase in both pores closing and interconnection. In the coating of 750 °C, the pores and particle interfaces in the as-sprayed coating have completely disappeared. Instead, the presence of a large number of equiaxed grains caused the original pores to be re-segmented, and a large number of submicron pores were visible between the equiaxed grains. The micropores could be generated in the healing of incomplete interfaces through the diffusion during annealing treatment (Ref 39).

Figure 8 shows the quasi-in situ microstructure of the coatings before and after 1100 °C heat treatment. Compared with the situation after heat treatment at 1000 °C, the coating structure further changed greatly. The residual morphology of spherical particles can be seen in the porous coating after heat treatment at 1000 °C (550-600 °C coating), but it was completely invisible after 1100 °C, and the coating structure was covered by a large number of plate-like (600 °C coating) and coarse equiaxed grains (700 and 750 °C coating). Significant penetration and expansion of the pores were observed in the 550 and 600 °C coatings. This may be caused by the rapid growth of the β phase and the large change in the structure when the temperature was close to the β-phase complete transition temperature at 1100 °C (Ref 40).

Porosity Evolution

In order to compare the trend of the porosity of the five coatings before and after the heat treatment, the porosity of the coatings after heat treatment at different temperatures was calculated by image analysis, and the results are shown in Fig. 9. In general, after heat treatment, the porosity of all

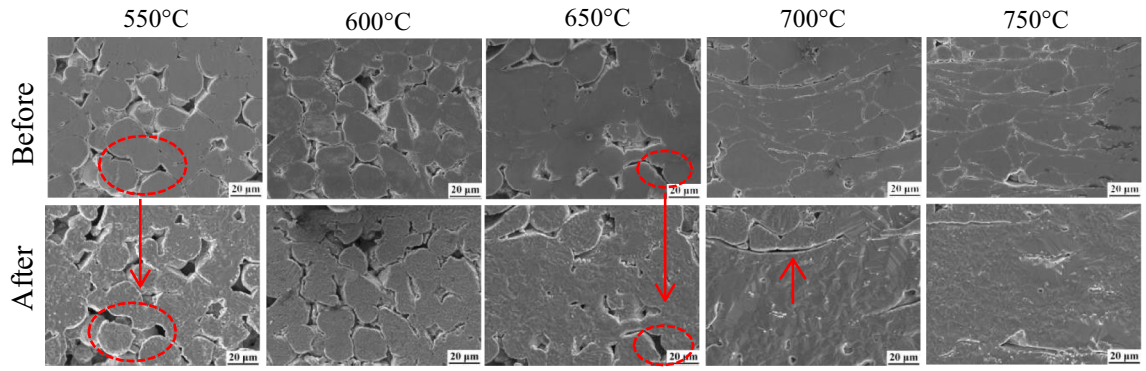

Fig. 6 Quasi-in situ observation of coatings before and after 900 °C heat treatment

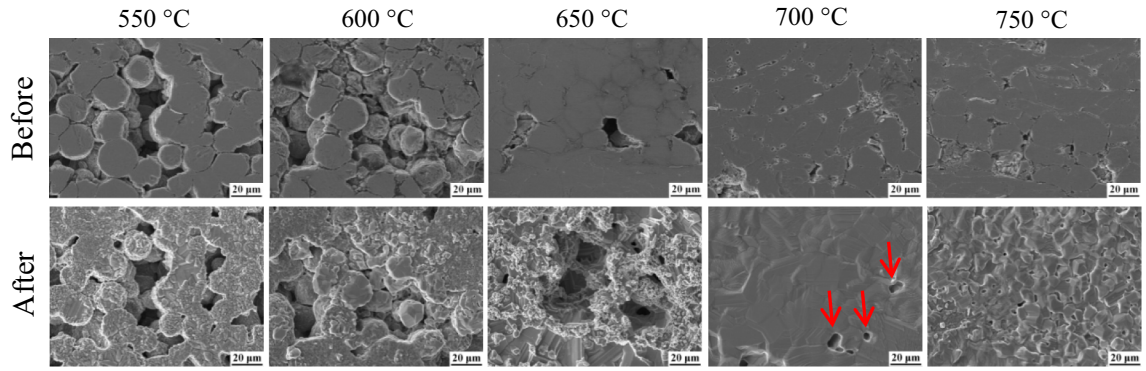

Fig. 7 Quasi-in situ observation of coatings before and after 1000 °C heat treatment

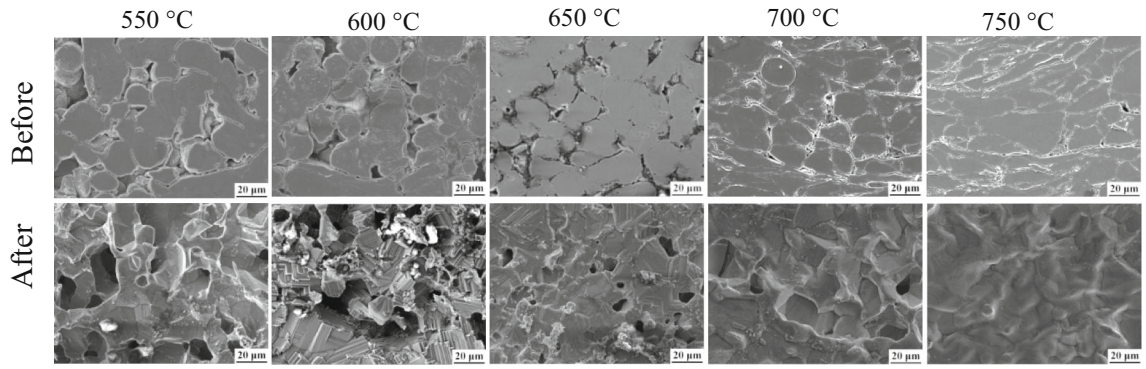

Fig. 8 Quasi-in situ observation of coatings before and after 1100 °C heat treatment

coatings reduced in varying degrees. As expected, the sintering effect dominated the heat treatment process, and the heat treatment promoted the densification of the TC4 coating, which has the potential to improve the mechanical properties of the coatings (Ref 41, 42). As observed by quasi-in situ observation, the porosity decrease after heat treatment at 600 °C was not substantial. The effect of diffusion and recrystallization after heat treatment at 700 °C was sent in the interface and disappearance of pores between particles, and there was a sharp drop in the porosity. After heat treatment at 800 °C, the decreasing trend was moderated, and the porosity increased abnormally in some coatings. When the temperature was increased to 900-1100 °C, an interesting phenomenon happened; the porosity of porous coatings (550-650 °C) increased, while that of dense coatings (700-750 °C) declined. As mentioned in the Introduction section, the decrease in porosity after heat treatment was reported in the thermal treatment of titanium alloy by cold spraying; it now seems that this is largely related to the porosity of the as-sprayed coating.

Residual Stress

The results of residual stress for the coating prepared at 550 °C in the original state and after heat treatment at 600 and 700 °C are shown in Table 2, which acted in the direction perpendicular to the spray direction. Due to the high-speed impact of particles during cold spraying, there was a large compressive residual stress in the as-sprayed coating, which is in agreement with literatures (Ref 43, 44). Moreover, the residual stress values differed by about 40 MPa in different directions, which is mainly due to the anisotropy of the cold spray coating (Ref 45). However, the residual stress in the coating was released during the heat treatment, and it dropped to 48 MPa at 600 °C, almost down about 80%. When the heat treatment temperature was further increased to 700 °C, the residual stress in the coating dropped to 18 MPa, and the decrease is about 93%. According to the previous quasi-in situ observation, it was known that the coating recrystallized at this temperature. As reported in the literature (Ref 46-48), the dynamic recovery and recrystallization can release stress, and the recrystallization process in the TC4 cold spray almost released almost all residual stress. Thus, it was assumed that when the temperature was further increased, the residual stress was completely released, almost close to zero. This relaxation was assumed to be resulting from two different factors, one of it being the yield strength reduction when exposed at high temperature and the other from the creep strain development during the holding stage (Ref 49).

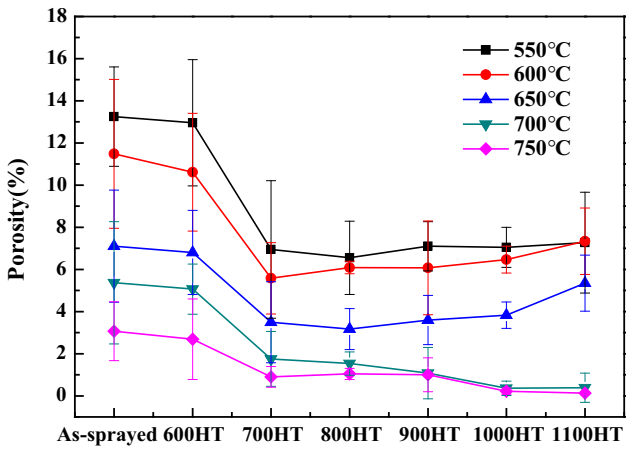

Fig. 9 Porosity of five coatings before and after heat treatment at different temperatures

Discussion

Shrinkage and Expansion Mechanism of Pores

From the quasi-in situ observation, the coating was densified during the heat treatment at 600-1100 °C, and the pores in the coating spheroidized and disappeared. At the same time, local expansion of the pores can also be observed, so the statistical results of the porosity of the coatings (prepared at 550-650 °C) increased at a certain temperature after decreasing. Since the porosity measurement with image analysis method and quasi-in situ observation were both based on a two-dimensional plane, on a cross section inside the coating, there will be two trends of pores shrinkage and expansion under thermal exposure. For the former, it was mainly due to the sintering effect (Ref 26, 50, 51). As reported in the literature, on account of adiabatic shear effect during the deposition of the cold spray coating (Ref 1), the metallurgical bond formed between the particles. During the heat treatment, the atoms on the face of the particles diffused to the contact area, resulting in necking. As a result, the metallurgical bonding of particles began to increase. With the increase in the temperature, the neck became thicker and the metallurgical bond increased more and more. So the center distance of the particles reduced, causing the shape of the pores among them to change from a star to a sphere under the action of surface tension (Ref 52). Due to the continuous shrinkage of the spherical pores, the pores eventually disappeared. Figure 10 shows the morphology of four closely packed particles observed on the fractural surface of a porous (prepared at 550 °C) coating after heat treatment at 800 °C. It was indicated that the increase in metallurgical bonding with the beginning of the necking formation between the particles was the internal mechanisms leading to the disappearance of the pores and the densification of the coating.

Table 2 Residual stress measured on TC4 coating prepared at 550 °C before and after heat treatment

Coating	In-plane principal residual stress σ_1, MPa	In-plane principal residual stress σ_2, MPa	Average in-plane residual stress σ, MPa
As-sprayed	− 222	− 263	− 242.5
600HT	− 47	− 49	− 48
700HT	− 17	− 19	− 18

On the other hand, pores expansion mechanism can be illustrated through a group of typical quasi-in situ contrast images before and after 900 °C heat treatment. As shown in Fig. 11, in some areas, the growth of pores between particles is seen, such as the pores between particles 1, 2, 3 and particle 4, and between particles 1′, 2′ and particles 3′, 4′ as well as between particles 3′ and 4′, 1″ and 2″. By contrast, it seemed that the pore expansion was caused by the movement of the particle to the particle nearby during the heat treatment. That is, the formation and growth of the neck between the particles made a part of pores shrink; at the same time, the movement of the particles caused by this process also brought about the growth of another part of the pores. According to the previous residual stress test results, there was a large compressive stress in the as-sprayed coating, which has an effect on the interfacial bonding of the coating. Studies have shown that the compressive stress present in the coating weakened the interface bonding (Ref 53) and promoted the coating to debond (Ref 54, 55). During the heat treatment of the coating, although the densification caused by thermal diffusion dominated the whole process, the residual stress existing in the original coating was released and caused partial particle interfaces to disengage inevitably. However, what kind of interface is easier to detach? The answer for that mainly resulted from the bonding situation in cold-sprayed coating (Ref 19, 29). As was generally accepted, metallurgical bonding and mechanical interlocking are two mechanisms of the metallic bonding in cold spraying (Ref 56, 57). In addition, Klinkov et al. (Ref 58) proposed "sticking" mechanism, which was derived from the Van der Waals or electrostatic forces. If the way of bonding between two particles is dominated by metallurgical bonding, it can be called "strong bonding," including areas that atoms can diffuse across the interface at the heat-treated temperature. While it is dominated by mechanical bonding and "sticking" bonding, where atoms cannot diffuse across the interface during heat treatment, it can be defined as "weak bonding," which also includes unbonded interfaces in the coating. For any particle in the coating, it will have "strong bonding" and "weak bonding" interfaces with the surrounding particles, and the atoms will preferentially diffuse to the "strong bonding" interfaces, since a high level of microstructural defects such as dislocations generated and piled up at these areas which can be involved in the interdiffusion enhancement (Ref 59-61). So the proportion of metallurgical bonding among these particles was enhanced. At the same time, interface detachment occurred on the other side of them inevitably, which were often the "weak bonding" interfaces. Then, the pores combination formed followed the detachment of these interfaces. Moreover, with the increase in heat treatment temperature, the shrinkage and the expansion of the pores occurred and continued simultaneously. (The schematic diagram is shown in Fig. 12.)

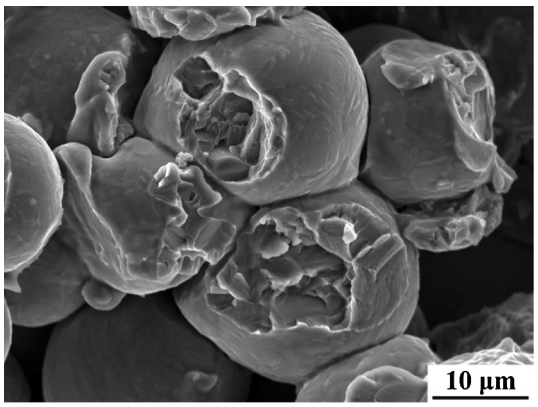

Fig. 10 Fracture morphology of the coating prepared at gas temperature of 550 °C after 800 °C heat treatment

Densification Mechanism of Coating

As was pointed out, the image analysis method can only measure the size of the pores in a two-dimensional surface of the coating and qualitatively estimate the porosity of the entire coating. Due to the resolution of this method, small two-dimensional pores, such as the pores between the weakly bonded interfaces which are usually submicron

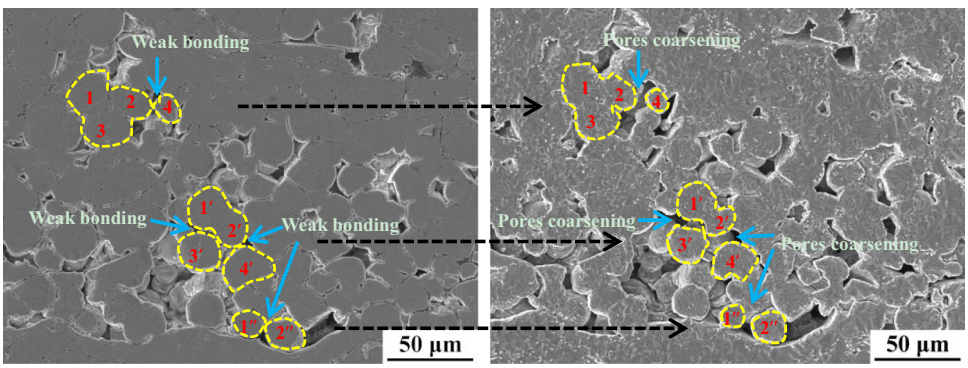

Fig. 11 Quasi-in situ observation of pores expansion in the coating prepared at 550 °C before and after heat treatment at 900 °C

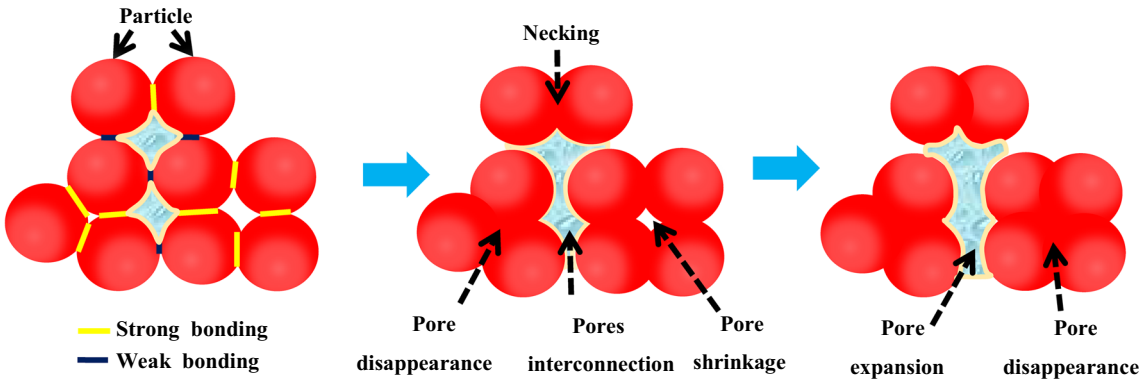

Fig. 12 Mechanism of pores shrinkage and expansion

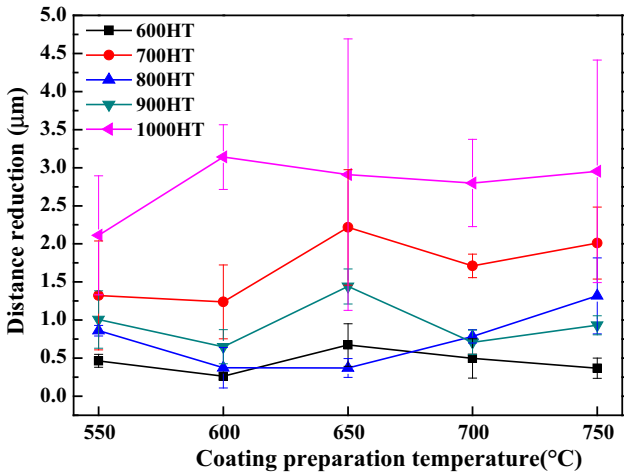

Fig. 13 Distance reduction per 100 micron after heat treatment

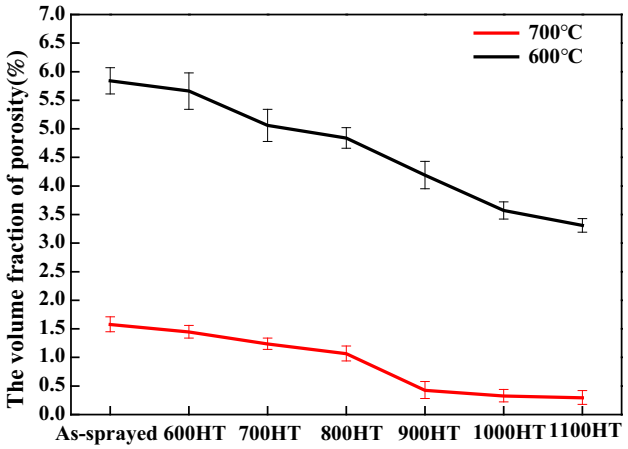

Fig. 14 Volume fraction of porosity for 600 °C and 700 °C coatings

size, cannot be distinguished frequently. So here it can be defined as "apparent porosity," which more reflects the form change of the pores. The detachment of weakly bonded interfaces on a surface will affect the "apparent porosity." However, the actual pores are three-dimensional and need to be measured by the total volume of the pores in the coating. Correspondingly, it also can be defined as "true porosity." Hussain et al. (Ref 23) used mercury intrusion porosimetry to characterize the interconnected porosity of cold-sprayed titanium coatings before and after heat treatment. It was found that there was a dramatic reduction in porosity because most of the pores mostly disappeared after heat treatment. Limited to experimental means, it was difficult to quantify the pore changes accurately in this study. Since the heat treatment was essentially a sintering process, it was speculated that the "true porosity" of the five coatings in this experiment should tend to decrease after heat treatment. In order to verify this conjecture, the distance difference before and after heat treatment was obtained by quasi-in situ measurement in the coating. As Fig. 13 shows, after heated at 600-1000 °C, all of the distances had decreased, that was to say, the volume of the coating shrank under thermal exposure, so the conclusion can be drawn that the "true porosity" always decreased during heat treatment in this study. Figure 14 shows the volume fraction of porosity in the coating prepared at 600 and 700 °C, which was obtained from Archimedes measurement. It can also be seen that "true porosity" was decreased both in the coating prepared at low temperature and in the one at high temperature.

So how did coating densification occur? As mentioned above, diffusion during heat treatment led to the formation of necking between particles, and continuous development of necking led to the mutual fusion between particles and the disappearance of interfacial pores. Just as the conclusion was drawn above, in essence, the bonding state of the particle interface in cold spraying directly determined the change of pores at high temperature. Suppose there was a parameter α, which is defined as the ratio of the strong bonding interfaces to the weak bonding interfaces in the as-sprayed coating. During the heat treatment, because of the formation of necking, the interface metallurgical bonding enhanced gradually. With the increase in temperature, the

fusion between particles increased, and the strong bonding interfaces were further enhanced. At the same time, weakly bonded interfaces were strengthened and transformed into strong bonding. Thus, α grew larger and larger; the continuation of this process led to the final densification of the coating. It is undeniable that there is interface separation in some area at high temperatures as showed in the cross section, but in a three-dimensional state, one particle bonded with many surrounding particles at the same time, and the detachment of one interface was accompanied by further fusion of other interfaces, and the connected three-dimensional particles do not shrink freely. Therefore, in general, during the sintering-dominated heat treatment process, the metallurgical bonding between the particles continued to increase, and pores constantly shrank and disappeared.

The Relation Between Porosity and Heat Treatment Temperature

The densification of the coating is related to diffusion and mass transfer mechanism, which is the root cause of the pores change. The diffusion of matter is heavily dependent on temperature, and increased atomic energy at high temperature can enhance diffusion. Therefore, the pores will change more as the temperature increases. According to the analysis above, for a two-dimensional cross section in the coating, the evolution of the pores with temperature had the trends of both shrinkage and expansion, and the "apparent porosity" based on two-dimensional statics was varying.

Figure 15 reveals the change trend of both "apparent porosity" and "true porosity" with the heat treatment temperature. Based on the previous analysis, the pore change of the cold spray coating during the heat treatment was closely related to the bonding state between particles in the as-sprayed coating. The less the weakly bonded particle interfaces were, the less likely the detachment of them. For "apparent porosity," there are two trends. For the coatings prepared at lower gas temperature (especially below 650 °C), when the heat treatment temperature is low, the diffusion is weak, so the particle movement is slight, and metallurgical bonding does not increase obviously while the weak bonding interfaces are not significantly separated because it has to overcome a certain barrier for interfaces detachment. This stage can be called "inoculation stage." After that, when the temperature increases to a certain value, especially when the coating recrystallization temperature is reached, the porosity drops rapidly. This stage can be called "quasi-free contraction stage." In this stage, shrinkage of small pores occurs first followed by larger ones, which results in a significant decrease in the porosity of the coating. Nevertheless, with the temperature increasing, the expansion of the pores caused by weakly bounded surfaces detachment is also increasing, when the expansion effect exceeds the contraction effect at a certain temperature, the coating porosity will rebound. This stage can be called "Arrested contraction stage." Apparent porosity will increase after decreasing in this stage. In addition, as the shrinkage and expansion of pores do not continue indefinitely, when the heat-treated temperature is high enough, the ability of atomic diffusivity will increase significantly; the connected three-dimensional particles do not prevent the shrink. So the porosity will decrease slowly and eventually become a bulk material. This stage can be called "Free contraction stage." However, for the coatings prepared at a higher gas temperature (especially above 700 °C), due to larger particle deformation, and as the possibility and degree of metallurgical bonding between the particles are greater than the coating prepared at a lower temperature, the detachment of particle interface during heat treatment is negligible. Thus, the rebound of the coating porosity cannot be caused, and the "apparent porosity" will be decreased continuously. When it comes to "true porosity," according to the analysis above, the diffusion will be enhanced with the increase in the temperature, so metallurgical bonding in the coating will be increased continuously, so the "true porosity" will decrease.

In addition, it should be noted that here we only consider the effect of original bonding state on the porosity of the coating. In the actual heat treatment process, phase transformation, grain growth, etc., all have effects on the pores (Ref 62). These need to be further analyzed in the future work.

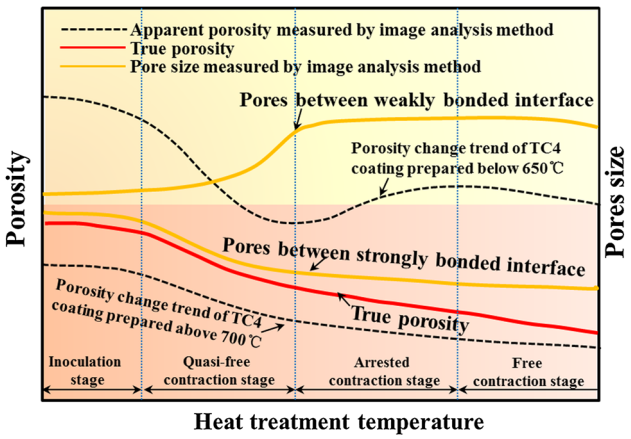

Fig. 15 Trend of porosity and pores size change with heat treatment temperature

Conclusions

In this study, five TC4 coatings were prepared using an in situ shot-peening-assisted cold spraying technology at different gas temperatures, and the effect of vacuum heat treatment temperature on the change of pores structure was evaluated. The main conclusions drawn from this study were as follows:

- When the coatings heat-treated at 600 °C, the microstructure did not change too much, and the interface between the particles was still obvious; when the heat treatment temperature was increased to 700 °C, the coating recrystallized and a large number of fine equiaxed grains appeared. The boundaries of the particles became blurred, and the pores appeared to be spheroidized and partially disappeared. When the temperature increased to 800 °C, the particle interface was further blurred, and the pores expansion and connectivity phenomenon occurred locally. When further rising heat temperature to 900-1100 °C, the expansion of pores in the coatings prepared at relatively low temperature was more obvious, and the coatings prepared at relatively high temperature became more and more dense with the heat treatment temperature increasing;
- The results of residual stress showed that there is a compressive stress of 242.5 MPa in as-sprayed coating, and the release of residual stress occurred during heat treatment and it released by 80 and 90% at 600 and 700 °C, respectively.
- By further analyzing the causes of pores structure changes, it was predicted that the state of bonding between the particles in the cold-sprayed coating determined the change of the pores during the heat treatment. For the coating prepared at low temperature, the particles deformed slightly, resulting in a large number of weakly bonded interfaces between the particles, and detachment occurred to these interfaces at a certain temperature due to release of the residual stress, followed by the increase in coating "apparent porosity." However, the coating prepared at high temperature has little interfacial detachment owing to improvement in particles bonding.
- The results of Archimedes volume fraction of porosity in the coating showed continuous densification occurred during heat treatment. So the "true porosity" of the coatings always decreased. The reason for this is the transformation of the weakly bonded interface to strongly bonded interface, and metallurgical bonding grew more and more around the same time as the pores turned to eliminate in this process.

Acknowledgments The authors would like to thank the financial support by the National Science Fund of China (No. 51761145108).

References

1. H. Assadi, F. Gartner, T. Stoltenhoff, and H. Kreye, Bonding Mechanism in Cold Gas Spraying, *Acta Mater.*, 2003, **51**(15), p 4379-4394
2. T. Stoltenhoff, C. Borchers, F. Gartner, and H. Kreye, Microstructures and Key Properties of Cold-Sprayed and Thermally Sprayed Copper Coatings, *Surf. Coat. Technol.*, 2006, **200**(16–17), p 4947-4960
3. D.L. Gilmore, R.C. Dykhuizen, R.A. Neiser, T.J. Roemer, and M.F. Smith, Particle Velocity and Deposition Efficiency in the Cold Spray Process, *J. Therm. Spray Technol.*, 1999, **8**(4), p 576-582
4. T. Hussain, D.G. McCartney, P.H. Shipway, and D. Zhang, Bonding Mechanisms in Cold Spraying: The Contributions of Metallurgical and Mechanical Components, *J. Therm. Spray Technol.*, 2009, **18**(3), p 364-379
5. M. Fukumoto, H. Wada, K. Tanabe, M. Yamada, E. Yamaguchi, A. Niwa, M. Sugimoto, and M. Izawa, Effect of Substrate Temperature on Deposition Behavior of Copper Particles on Substrate Surfaces in the Cold Spray Process, *J. Therm. Spray Technol.*, 2007, **16**(5–6), p 643-650
6. P. Jakupi, P.G. Keech, I. Barker, S. Ramamurthy, R.L. Jacklin, D.W. Shoesmith, and D.E. Moser, Characterization of Commercially Cold Sprayed Copper Coatings and Determination of the Effects of Impacting Copper Powder Velocities, *J. Nucl. Mater.*, 2015, **466**, p 1-11
7. W.-Y. Li, H. Liao, C.-J. Li, H.-S. Bang, and C. Coddet, Numerical Simulation of Deformation Behavior of Al Particles Impacting on Al Substrate and Effect of Surface Oxide Films on Interfacial Bonding in Cold Spraying, *Appl. Surf. Sci.*, 2007, **253**(11), p 5084-5091
8. T. Wojdat, M. Winnicki, M. Rutkowska-Gorczyca, S. Krupiński, and K. Kubica, Soldering Aluminium to Copper with the Use of Interlayers Deposited by Cold Spraying, *Arch. Civil Mech. Eng.*, 2016, **16**(4), p 835-844
9. C.-J. Li, W.-Y. Li, and Y.-Y. Wang, Formation of Metastable Phases in Cold-Sprayed Soft Metallic Deposit, *Surf. Coat. Technol.*, 2005, **198**(1–3), p 469-473
10. X.-T. Luo, Y.-K. Wei, Y. Wang, and C.-J. Li, Microstructure and Mechanical Property of Ti and Ti6Al4V Prepared by an In Situ Shot Peening Assisted Cold Spraying, *Mater. Des.*, 2015, **85**, p 527-533
11. N.W. Khun, A.W.Y. Tan, K.J.W. Bi, and E. Liu, Effects of Working Gas on Wear and Corrosion Resistances of Cold Sprayed Ti-6Al-4V Coatings, *Surf. Coat. Technol.*, 2016, **302**, p 1-12
12. M.V. Vidaller, A. List, F. Gaertner, T. Klassen, S. Dosta, and J.M. Guilemany, Single Impact Bonding of Cold Sprayed Ti-6Al-4V Powders on Different Substrates, *J. Therm. Spray Technol.*, 2015, **24**(4), p 644-658
13. A. Chaudhuri, Y. Raghupathy, D. Srinivasan, S. Suwas, and C. Srivastava, Microstructural Evolution of Cold-Sprayed Inconel 625 Superalloy Coatings on Low Alloy Steel Substrate, *Acta Mater.*, 2017, **129**, p 11-25
14. P. Cavaliere, A. Silvello, N. Cinca, H. Canales, S. Dosta, I. Garcia Cano, and J.M. Guilemany, Microstructural and Fatigue Behavior of Cold Sprayed Ni-based Superalloys Coatings, *Surf. Coat. Technol.*, 2017, **324**, p 390-402
15. R. Singh, K.H. Rauwald, E. Wessel, G. Mauer, S. Schruefer, A. Barth, S. Wilson, and R. Vassen, Effects of Substrate Roughness

and Spray-Angle on Deposition Behavior of Cold-Sprayed Inconel 718, *Surf. Coat. Technol.*, 2017, **319**, p 249-259
16. A.R. Toibah, M. Sato, M. Yamada, and M. Fukumoto, Cold-Sprayed TiO2 Coatings from Nanostructured Ceramic Agglomerated Powders, *Mater. Manuf. Processes*, 2016, **31**(11), p 1527-1534
17. K. Ravi, Y. Ichikawa, K. Ogawa, T. Deplancke, O. Lame, and J.-Y. Cavaille, Mechanistic Study and Characterization of Cold-Sprayed Ultra-High Molecular Weight Polyethylene-Nano-Ceramic Composite Coating, *J. Therm. Spray Technol.*, 2015, **25**(1–2), p 160-169
18. G.-R. Li and L.-S. Wang, Durable TBCs with Self-Enhanced Thermal Insulation Based on Co-Design on Macro-and Microstructure. *Appl. Surf. Sci.*, 2019, **483**, p 472-480
19. C.-J. Li and W.-Y. Li, Deposition Characteristics of Titanium Coating in Cold Spraying, *Surf. Coat. Technol.*, 2003, **167**(2–3), p 278-283
20. T. Marrocco, D.G. McCartney, P.H. Shipway, and A.J. Sturgeon, Production of Titanium Deposits by Cold-Gas Dynamic Spray: Numerical Modeling and Experimental Characterization, *J. Therm. Spray Technol.*, 2006, **15**(2), p 263-272
21. B.N. Kim, K. Hiraga, K. Morita, H. Yoshida, and H. Zhang, Diffusive Model of Pore Shrinkage in Final-Stage Sintering Under Hydrostatic Pressure, *Acta Mater.*, 2011, **59**(10), p 4079-4087
22. G. Sundararajan, N.M. Chavan, and S. Kumar, The Elastic Modulus of Cold Spray Coatings: Influence of Inter-Splat Boundary Cracking, *J. Therm. Spray Technol.*, 2013, **22**(8), p 1348-1357
23. T. Hussain, D.G. McCartney, P.H. Shipway, and T. Marrocco, Corrosion Behavior of Cold Sprayed Titanium Coatings and Free Standing Deposits, *J. Therm. Spray Technol.*, 2010, **20**(1–2), p 260-274
24. M.A. Garrido, P. Sirvent, and P. Poza, Evaluation of Mechanical Properties of Ti6Al4V Cold Sprayed Coatings, *Surf. Eng.*, 2017, **34**(5), p 399-406
25. W.-Y. Li, C. Zhang, X. Guo, J. Xu, C.-J. Li, H. Liao, C. Cocidet, and K.A. Khor, Ti and Ti-6Al-4V Coatings by Cold Spraying and Microstructure Modification by Heat Treatment, *Adv. Eng. Mater.*, 2007, **9**(5), p 418-423
26. P. Vo, E. Irissou, J.G. Legoux, and S. Yue, Mechanical and Microstructural Characterization of Cold-Sprayed Ti-6Al-4V After Heat Treatment, *J. Therm. Spray Technol.*, 2013, **22**(6), p 954-964
27. I.C. Noyan and J.B. Cohen, *Determination of strain and stress fields by diffraction methods, Residual Stressed.*, Springer, Berlin, 1987, p 117-163
28. Y.-C. Yang and E. Chang, Influence of Residual Stress on Bonding Strength and Fracture of Plasma-Sprayed Hydroxyapatite Coatings on Ti-6Al-4V Substrate, *Biomaterials*, 2001, **22**(13), p 1827-1836
29. S.H. Zahiri, D. Fraser, and M. Jahedi, Recrystallization of Cold Spray-Fabricated CP Titanium Structures, *J. Therm. Spray Technol.*, 2008, **18**(1), p 16-22
30. H.R. Salimijazi, Z.A. Mousavi, M.A. Golozar, J. Mostaghimi, and T. Coyle, Kinetic Study of the Solid-State Transformation of Vacuum-Plasma-Sprayed Ti-6Al-4V Alloy, *J. Therm. Spray Technol.*, 2013, **23**(1–2), p 31-39
31. R. Huang, M. Sone, W. Ma, and H. Fukanuma, The Effects of Heat Treatment on the Mechanical Properties of Cold-Sprayed Coatings, *Surf. Coat. Technol.*, 2015, **261**, p 278-288
32. B. Al-Mangour, R. Mongrain, E. Irissou, and S. Yue, Improving the Strength and Corrosion Resistance of 316L Stainless Steel for Biomedical Applications Using Cold Spray, *Surf. Coat. Technol.*, 2013, **216**, p 297-307
33. N. Kang, P. Coddet, H. Liao, and C. Coddet, Cold Gas Dynamic Spraying of a Novel Micro-Alloyed Copper: Microstructure, Mechanical Properties, *J. Alloy. Compd.*, 2016, **686**, p 399-406
34. S. Kumar and A.A. Rao, Influence of Coating Defects on the Corrosion Behavior of Cold Sprayed Refractory Metals, *Appl. Surf. Sci.*, 2017, **396**, p 760-773
35. T. Liu, X.-T. Luo, X. Chen, G.-J. Yang, C.-X. Li, and C.-J. Li, Morphology and Size Evolution of Interlamellar Two-Dimensional Pores in Plasma-Sprayed La 2 Zr 2 O 7 Coatings During Thermal Exposure at 1300 °C, *J. Therm. Spray Technol.*, 2015, **24**(5), p 739-748
36. P. Vo, D. Goldbaum, W. Wong, E. Irissou, J.-G. Legoux, R.R. Chromik, and S. Yue, Cold-Spray Processing of Titanium and Titanium Alloys, *Titanium Powder Metallurgy*, 2015, p 405-423
37. W.-Y. Li, C. Yang, and H. Liao, Effect of Vacuum Heat Treatment on Microstructure and Microhardness of Cold-Sprayed TiN Particle-Reinforced Al Alloy-Based Composites, *Mater. Des.*, 2011, **32**(1), p 388-394
38. N.W. Khun, A.W.Y. Tan, W. Sun, and E. Liu, Effect of Heat Treatment Temperature on Microstructure and Mechanical and Tribological Properties of Cold Sprayed Ti-6Al-4V Coatings, *Tribol. Trans.*, 2016, **60**(6), p 1033-1042
39. C.-J. Li, W.-Y. Li, and H. Liao, Examination of the Critical Velocity for Deposition of Particles in Cold Spraying, *J. Therm. Spray Technol.*, 2006, **15**(2), p 212-222
40. F.J. Gil and J.A. Planell, Behaviour of Normal Grain Growth Kinetics in Single Phase Titanium and Titanium Alloys, *Mater. Sci. Eng. Struct. Mater. Prop. Microstruct. Process.*, 2000, **283**(1–2), p 17-24
41. Y.J. Li, X.T. Luo, H. Rashid, and C.J. Li, A new Approach to Prepare Fully Dense Cu with High Conductivities and Anti-Corrosion Performance by Cold Spray, *J. Alloys Compd.*, 2018, **740**, p 406-413
42. A. Singh, G. Singh, and V. Chawla, Influence of Post Coating Heat Treatment on Microstructural, Mechanical and Electrochemical Corrosion Behaviour of Vacuum Plasma Sprayed Reinforced Hydroxyapatite Coatings, *J. Mech. Behav. Biomed. Mater.*, 2018, **85**, p 20-36
43. R. Ghelichi, S. Bagherifard, D. MacDonald, I. Fernandez-Pariente, B. Jodoin, and M. Guagliano, Experimental and Numerical Study of Residual Stress Evolution in Cold Spray Coating, *Appl. Surf. Sci.*, 2014, **288**, p 26-33
44. Z. Arabgol, H. Assadi, T. Schmidt, F. Gärtner, and T. Klassen, Analysis of Thermal History and Residual Stress in Cold-Sprayed Coatings, *J. Therm. Spray Technol.*, 2014, **23**(1–2), p 84-90
45. K. Yang, W. Li, X. Yang, and Y. Xu, Anisotropic Response of Cold Sprayed Copper Deposits, *Surf. Coat. Technol.*, 2018, **335**, p 219-227
46. V. Luzin, K. Spencer, and M.-X. Zhang, Residual Stress and Thermo-Mechanical Properties of Cold Spray Metal Coatings, *Acta Mater.*, 2011, **59**(3), p 1259-1270
47. B.R. Sridhar, G. Devananda, K. Ramachandra, and R. Bhat, Effect of Machining Parameters and Heat Treatment on the Residual Stress Distribution in Titanium Alloy IMI-834, *J. Mater. Process. Technol.*, 2003, **139**(1–3), p 628-634
48. K.A. Venkata, S. Kumar, H.C. Dey, D.J. Smith, P.J. Bouchard, and C.E. Truman, Study on the Effect of Post Weld Heat Treatment Parameters on the Relaxation of Welding Residual Stresses in Electron Beam Welded P91 Steel Plates, *Procedia Eng.*, 2014, **86**(86), p 223-233
49. P. Dong, S. Song, and J. Zhang, Analysis of Residual Stress Relief Mechanisms in Post-Weld Heat Treatment, *Int. J. Press. Vessels Pip.*, 2014, **122**(1), p 6-14
50. Y.Q. Ren, P.C. King, Y.S. Yang, T.Q. Xiao, C. Chu, S. Gulizia, and A.B. Murphy, Characterization of Heat Treatment-Induced

Pore Structure Changes in Cold-Sprayed Titanium, *Mater. Charact.*, 2017, **132**, p 69-75
51. W.L.H.L.C. Coddet, Preparation and Characterization of Porous Titanium and Titanium Alloy by Cold Spraying, *Rare Metal Mater. Eng.*, 2009, **38**, p 260-263
52. J.L. Shi and Z.X. Lin, The Flow Characteristics of Hot-Pressing of Beta-AL2O3, *Ceram. Int.*, 1989, **15**(2), p 107-112
53. YungChin Yang, Influence of Residual Stress on Bonding Strength of the Plasma-Sprayed Hydroxyapatite Coating After the Vacuum Heat Treatment, *Surf. Coat. Technol.*, 2007, **201**(16), p 7187-7193
54. A.G. Evans, G.B. Crumley, and R.E. Demaray, On the Mechanical Behavior of Brittle Coatings and Layers, *Oxid. Met.*, 1983, **20**(5–6), p 193-216
55. Y.C. Yang and E. Chang, Influence of Residual Stress on Bonding Strength and Fracture of Plasma-Sprayed Hydroxyapatite Coatings on Ti-6Al-4V Substrate, *Biomaterials*, 2001, **22**(13), p 1827-1836
56. C. Chen, Y. Xie, S. Yin, M.P. Planche, S. Deng, R. Lupoi, and H. Liao, Evaluation of the Interfacial Bonding Between Particles and Substrate in Angular Cold Spray, *Mater. Lett.*, 2016, **173**, p 76-79
57. W.Y. Li, C. Zhang, H.T. Wang, X.P. Guo, H.L. Liao, C.J. Li, and C. Coddet, Significant Influences of Metal Reactivity and Oxide Films at Particle Surfaces on Coating Microstructure in Cold Spraying, *Appl. Surf. Sci.*, 2007, **253**(7), p 3557-3562
58. S.V. Klinkov, V.F. Kosarev, and M. Rein, Cold Spray Deposition: Significance of Particle Impact Phenomena, *Aerosp. Sci. Technol.*, 2005, **9**(7), p 582-591
59. B.B. Khina, I. Solpan, and G.F. Lovshenko, Modelling Accelerated Solid-State Diffusion Under the Action of Intensive Plastic Deformation, *J. Mater. Sci.*, 2004, **39**(16–17), p 5135-5138
60. X.T. Luo, C.X. Li, F.L. Shang, G.J. Yang, Y.Y. Wang, and C.J. Li, High Velocity Impact Induced Microstructure Evolution During Deposition of Cold Spray Coatings: A Review, *Surf. Coat. Technol.*, 2014, **254**(10), p 11-20
61. A.L. Ruoff, Enhanced Diffusion During Plastic Deformation by Mechanical Diffusion, *J. Appl. Phys.*, 1967, **38**(10), p 3999-4003
62. J.A. Varela, O.J. Whittemore, and E. Longo, Pore Size Evolution During Sintering of Ceramic Oxides, *Ceram. Int.*, 1990, **16**(3), p 177-189